buildings

MDPI

Article

Determination of Tensile Strength at Crack Initiation in Dynamic Brazilian Disc Test for Concrete-like Materials

Jie Wang [1,2] and Junlin Tao [2,3,*]

[1] School of Mechanical Engineering, Nanjing University of Science and Technology, Nanjing 210094, China; wangjie19@gscaep.ac.cn
[2] Institute of Systems Engineering, China Academy of Engineering Physics, Mianyang 621900, China
[3] School of Civil Engineering and Architecture, Southwest University of Science and Technology, Mianyang 621010, China
* Correspondence: junlintao19@126.com

Abstract: Concrete is a brittle material whose tensile strength is about one-tenth of its compressive strength. Tensile strength is a key parameter for concrete under impact loading. When a turning point occurs before peak load in the load–time curve from the dynamic Brazilian disc test, there is no basis for choosing the turning point or the peak load to calculate the tensile strength. The objective of this study is determining the crack initiation tensile stress at the turning point or the peak. The method contrasts the time duration from Digital image correlation (DIC) and the load–time curve from a split Hopkinson pressure bar (SHPB) system in order to obtain the load value when cracking first appears. The crack initiation tensile strength is less than the peak strength for concrete specimens with a turning point in the load–time curve. The crack initiation tensile strength is equal to the peak strength for concrete specimens without a turning point in the load–time curve. The proposed method is successfully applied to determine crack initiation of concrete specimens and obtain tensile strength at crack initiation of concrete specimens.

Keywords: crack initiation tensile strength; Brazilian disc test; DIC; SHPB; concrete; load–time curve; peak strength

Citation: Wang, J.; Tao, J. Determination of Tensile Strength at Crack Initiation in Dynamic Brazilian Disc Test for Concrete-like Materials. *Buildings* **2022**, *12*, 797. https://doi.org/10.3390/buildings12060797

Academic Editor: Antonio Caggiano

Received: 11 May 2022
Accepted: 7 June 2022
Published: 10 June 2022

1. Introduction

Stress-induced crack initiation is a precursor to the failure of brittle materials such as concrete and rock. The increase of stress will eventually destroy underground excavation projects and infrastructure facilities. A better estimation of crack initiation is critical to reveal the deformation and stability of the brittle material, and it is also very beneficial to engineering design and applications [1].

Crack evolution of brittle materials can be divided into crack initiation, crack propagation, and crack coalescence. In the process of crack evolution, the determination of crack initiation stress is the key. Many scholars put forward a series of methods, such as volumetric strain method [2,3], energy dissipation method [1], lateral strain method [4], crack volumetric strain method [5], lateral strain response method [6], relative compression strain response method [7], and acoustic emission method [8], to obtain crack initiation of brittle materials under compression load. With the help of these methods to determine crack initiation, some empirical formulas [7,9,10] on crack initiation stress under compression load have been proposed one by one. The crack initiation strength is lower than the peak compressive strength from the empirical formulas. Li X et al. [10] summarized a total of 953 compressive tests from relevant references and found the crack initiation stress to the peak compressive strength of about 0.48. Nicksiar et al. [6] suggested to promulgating a standard for determining the crack initiation stress. It can be seen that it is significant to acquire the crack initiation stress of brittle materials.

Tensile strength is lower than compression strength for brittle materials. Meanwhile, the tensile failure is one of the main reasons for the damage of concrete structures in bridges, underground construction, office buildings, etc. Therefore, it is also vital to determine crack initiation stress under tensile load.

The Brazilian disc test, which is commended by The International Society for Rock Mechanics (ISRM) and American Society for Testing Material (ASTM) standards [11–13], is an indirect method to obtain tensile strength of brittle materials, such as concrete and rock. For the static Brazilian disc test, strain gauges, extensometers and acoustic emission technology, high-speed camera, and DIC technology were employed to obtain crack evolution of brittle materials. Wei et al. [14] conducted the active and passive ultrasonic technique and found the crack initiation points of the sandstone specimen occurred away from the center of the disc. Guo et al. [15] acquired curves of crack width of plain concrete with time by the means of an extensometer and found the crack width increased rapidly when the load force was close to its peak value. Aliabadian et al. [16] found that the cracks detectable by DIC appeared when the load force of sandstone specimen reached its peak. Sharafisafa et al. [17] employed DIC to obtain maximum principal strain at the center of the block-in-matrix rock specimen and found a tensile crack initiated when the load reached its peak value. The crack initiation tensile stress was almost equal to the peak tensile strength in the static Brazilian disc test [18].

For the dynamic Brazilian disc test, strain gauges, high-speed camera, and DIC technology were utilized to determine the crack evolution of brittle materials. Wang et al. [19] measured the crack initiation and crack propagation velocity through strain gauges glued in front of the crack tip of the specimen. Zhou et al. [20] combined high-speed photography with strain gauges to study the crack process of granite specimens. Ai et al. [21] extracted cracking behavior from images and analyzed quantitatively the relationship between impact velocity, crack velocity, and dynamic mechanical properties. Full-field strain evolution and the whole process of crack initiation, propagation, and failure of brittle materials [22,23] were captured by DIC. The above approaches mainly focus on the crack propagation evolution, and are rarely concerned with crack initiation tensile stress in the dynamic Brazilian disc test.

In addition, in the dynamic Brazilian disc test, when the load–time curve appears a turning point before the peak load [24,25], there is no basis for choosing the load at the turning point or the peak to calculate the tensile strength. Determination of crack initiation at the turning point or the peak is crucial to distinguish crack initiation tensile strength and peak tensile strength. In this study, a method is proposed to investigate the crack initiation and the crack evolution of concrete specimens in the dynamic Brazilian disc test. This proposed method combines the DIC technology with the load–time curve to acquire the tensile stress at the onset of cracking. The crack initiation tensile strength and the peak tensile strength are measured by the proposed method. The images of crack evolution and responding to the load–time curve is analyzed.

2. Specimen Preparation and Experimental Setups

2.1. Specimen Preparation

According to the relevant regulation of "Specification for mix proportion design of ordinary concrete (JGJ55-2011)" [26], the concrete is designed to be C30 strength grade (the 28-day cube compression strength of 30 MPa). The mix proportion for concrete is shown in Table 1. The raw materials for concrete are as follows: the cement is selected from P.C 42.5R grade ordinary Portland cement, and its density is 2900 kg/m^3, and setting time is 50 min; the fine aggregate is natural river sand with a fineness modulus of 2.8; the coarse aggregate is the crushed stone with a particle size of 5–20 mm, and its apparent density is 2410 kg/m^3, and the bulk density is 1370 kg/m^3, and water absorption is 0.6%. The diameter of the split Hopkinson pressure bar employed for the dynamic test is 120 mm. Consequently, the size of the concrete specimens used in the dynamic Brazilian disc test is

designed to be Φ120 × 100 mm (120 mm diameter × 100 mm long) in this study. A total of 10 cylindrical concrete specimens were fabricated for the dynamic Brazilian disc test.

Table 1. The mix proportion for per cubic meter concrete (kg).

Cement	Fine Aggregate	Coarse Aggregate	Water
310	701	1194	195

2.2. Digital Image Correlation

In order to quantitatively measure the surface deformation of concrete specimens, apparatus including strain gauges, extensometers have been used in previous research. These tools are effective in measuring small amounts of deformation localized region but could not acquire whole development processes of full-field strain and failure mode. DIC technology does not suffer from these restrictions and has numerous other advantages comprising non-contact, full-field, low cost and efficiency. With the development of high-speed cameras and the correlation algorithm, DIC technology has been successfully used to obtain full-field deformation in different fields [27–29].

In DIC technology, the displacement and strain of the materials are calculated by comparing a series of digital images of the sample surface at different deformation stages, and by tracking the pixel movement of the region of interest. The test sample surface must have a random speckle pattern as a carrier of deformation [30]. In this study, as the concrete samples did not have a clear inherent speckle pattern, the surface of the concrete specimen was painted entirely white as the background, and artificial random black speckles were decorated on the surface for subsequent comparison and matching [17]. A high-speed camera system was employed to obtain high-quality images. The frame frequency was 30,000 fps, and the resolution was set as 512 × 384 to observe the dynamic failure process of concrete specimens.

The first image is called the reference image; the second and subsequent images in the loading condition are called the deformed images. DIC technique tracks a subset of several pixel points in the reference image and the deformed images. The displacement of the subset center point O, u, and v is obtained by employing the zero-normalized cross-correlation function [23,31]:

$$C(X) = \frac{\sum_{i=1}^{m}\sum_{j=1}^{m}\left[f(x_i, y_j) - \overline{f}\right] \cdot \left[g\left(x_i', y_j'\right) - \overline{g}\right]}{\sqrt{\sum_{i=1}^{m}\sum_{j=1}^{m}\left[f(x_i, y_j) - \overline{f}\right]^2} \cdot \sqrt{\sum_{i=1}^{m}\sum_{j=1}^{m}\left[g\left(x_i', y_j'\right) - \overline{g}\right]^2}} \tag{1}$$

$$\begin{cases} x_i' = x_i + u + \frac{\partial u}{\partial x}\Delta x + \frac{\partial u}{\partial y}\Delta y \\ y_i' = y_i + v + \frac{\partial v}{\partial x}\Delta x + \frac{\partial v}{\partial y}\Delta y \end{cases} \tag{2}$$

where $f(x, y)$ is grey intensity of the subset at the coordinates (x, y) in the reference image; $g(x', y')$ is grey intensity of the subset at the coordinates (x', y') in the deformed image; $\overline{f}$ and $\overline{g}$ represent average grey values of the reference image and the deformed image, respectively.

2.3. Split Hopkinson Pressure Bar

The dynamic Brazilian test using a split Hopkinson pressure bar (SHPB) system is a convenient means of determining the tensile strength of brittle materials [15,32,33]. In this study, a Split Hopkinson pressure bar (SHPB) system mainly composed of a high-pressure gas gun, a striker bar (600 mm in length), an incident bar (4000 mm in length), a transmission bar (4000 mm in length), data acquisition systems, and damping devices. The bars are made of aluminum alloy with a diameter of 120 mm, the Young's modulus is 72 GPa, and the yield strength is 300 MPa. The schematic diagram of the device is shown in Figure 1a.

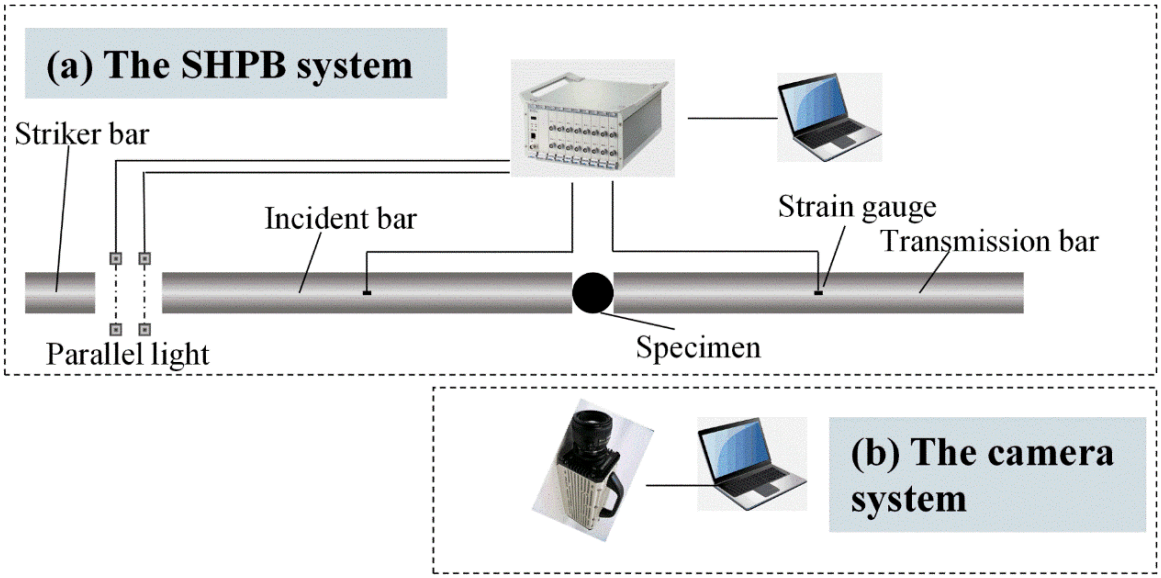

Figure 1. (**a**) the SHPB system, (**b**) the camera system.

In the dynamic Brazilian disk test, the striker bar hits the incident bar, forming an incident wave pulse $\varepsilon_i(t)$ in the incident bar. When the incident wave pulse propagates to the interface between the incident bar and the specimen, one part of the incident wave pulse will reflect on the interface to form a reflected wave pulse $\varepsilon_r(t)$ in the incident bar, and the other incident wave pulse will enter the transmission bar to form a transmitted wave pulse $\varepsilon_t(t)$. The strain gauges attached to the bars record the wave pulse signals. According to the one-dimensional elastic stress wave theory, the forces acting on the interfaces between the bars and the specimen can be calculated by the following formula [34].

$$F_1(t) = E[\varepsilon_i(t) + \varepsilon_r(t)]A \tag{3}$$

$$F_2(t) = E\varepsilon_t(t)A \tag{4}$$

where $F_1(t)$ and $F_2(t)$ are the forces acting on both ends of the specimen, E denotes the young's modulus of the incident bar and the transmission bar, A represents the cross-section area of the bars.

The necessary prerequisite for a valid dynamic Brazilian disc test is equilibrium of stress:

$$\varepsilon_i(t) + \varepsilon_r(t) = \varepsilon_t(t) \tag{5}$$

The static tensile strength of the concrete specimen shall be calculated by the following formula [35]:

$$\sigma_T = \frac{2F}{\pi DH} \tag{6}$$

where σ_T denotes static tensile strength, F represents the forces acting on both ends of the specimen, D and H are the diameter and height of the specimen, respectively.

In dynamic Brazilian disc test, once equilibrium of stress is fulfilled, the expression for the tensile strength based on the static tensile strength formula, i.e., $\sigma_T = \frac{2F}{\pi DH}$, can be used to estimate the dynamic tensile strength, with the force calculated from the transmitted strain [36,37].

$$\sigma_{TD} = \frac{2F_2(t)}{\pi DH} = \frac{2EA\varepsilon_t(t)}{\pi DH} \tag{7}$$

where σ_{TD} is dynamic tensile stress.

Equilibrium of stress at the transmitted bar/specimen and the incident bar/specimen interfaces is a necessary prerequisite for a valid Brazilian disc test under impact load. Thus, the stress at the contacts of bars is plotted to check the validity of the dynamic

Brazilian disc test. As shown in Figure 2, the curve $\varepsilon_t(t)$ coincides well with the curve $\varepsilon_i(t) + \varepsilon_r(t)$. The equilibrium condition of the stress at the contacts of bars is met, which indicates the dynamic Brazilian disc test is valid and the experimental result is reliable. In the present study, the load–time curve and the dynamic tensile stress of concrete specimens are calculated by Equation (4) and Equation (7), respectively.

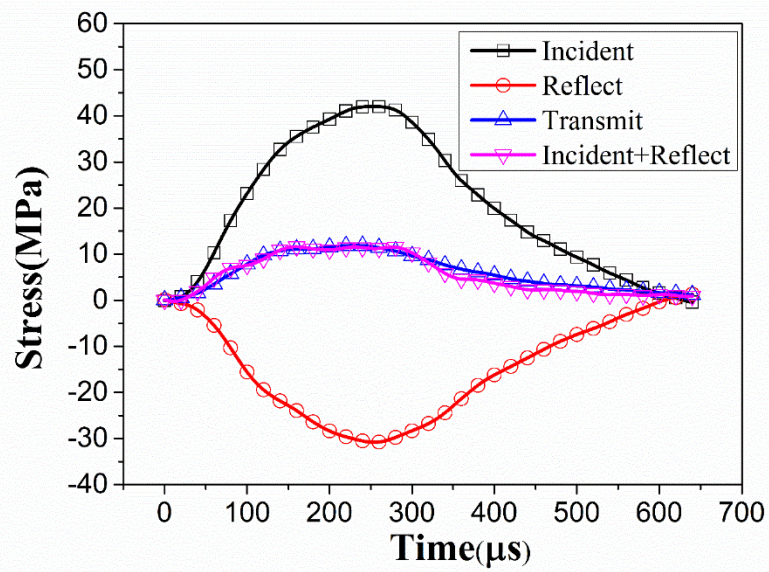

Figure 2. Stress equilibrium of typical concrete specimen.

3. Methods

In the dynamic Brazilian disc test, the SHPB system records the load–time curves of the concrete samples and the high-speed camera system obtains the images of crack evolution, such as crack initiation, crack propagation, and crack coalescence. However, the SHPB system and the high-speed camera system work independently, as shown in Figure 1. It is a tough problem that how to correspond the crack evolution, such as crack initiation, to the load–time curve one by one, so as to find the corresponding load during the specimen crack initiation. This study solves the problem and obtains the load value when cracking first appears.

A total of ten concrete specimens were tested at same impact velocity in the dynamic Brazilian disc test. the load–time curves of the concrete specimens can be calculated by Equation (4). The velocity of the striker bar is about 5.5 m/s. The number of concrete specimens whose load increases with time until the load force reaches its peak value in the load–time curves is seven. Figure 3a presents the load–time curve for one of the seven concrete specimens. Nevertheless, in the remaining three concrete specimens, there is a turning point before the load force reaches its peak value in the load–time curves, as shown in Figure 4a. Figures 3b and 4b illustrate that the stress equilibrium is met for a valid dynamic Brazilian disc test and the experimental result is reliable. In this study, the load–time curves of concrete specimens can be divided into two categories according to whether there is a turning point before the peak load, i.e., load–time curve with a turning point and load–time curve without a turning point.

The solid lines in Figures 2, 3b and 4b come from SHPB. The sampling frequency of SHPB is 1 M Hz. Thus, the number of data points of the solid lines is about 650, which is enough to describe the solid lines.

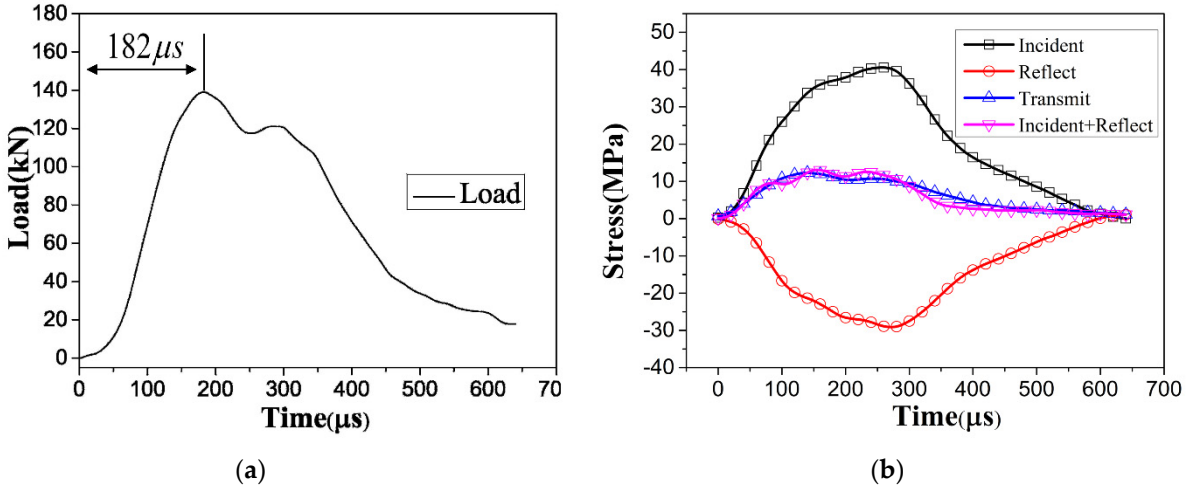

Figure 3. Load–time curve without a turning point. (**a**) Load–time curve, (**b**) equilibrium of stress.

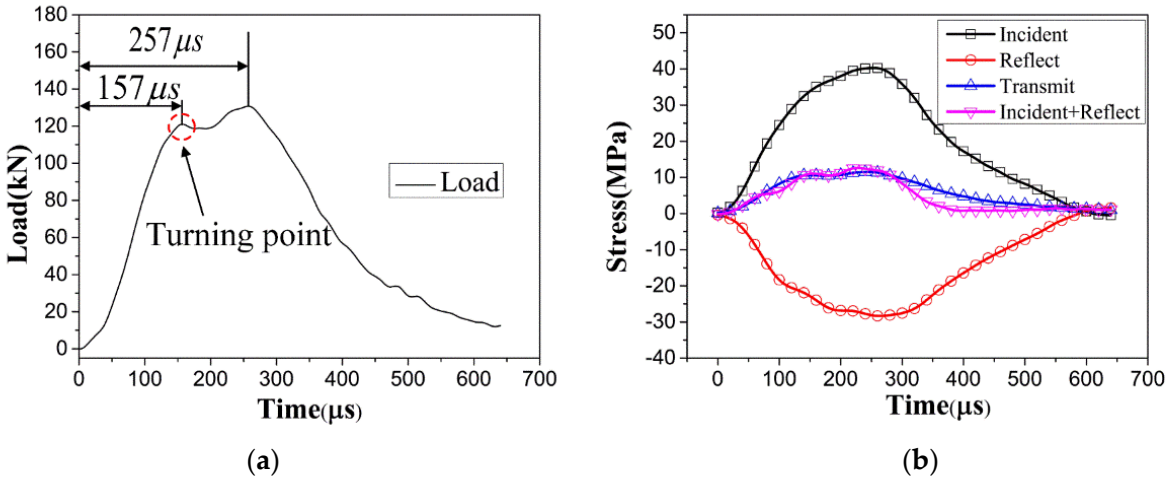

Figure 4. Load–time curve with a turning point. (**a**) Load–time curve, (**b**) equilibrium of stress.

The phenomenon of a turning point in the load–time is also present in Refs. [24,25]. In dynamic Brazilian disc test, Figure 5 shows a turning point before the peak load in the load–time curve from Ref. [24] and indicates that a turning point may appear before the peak load in the load–time curve at different loading speeds. Concrete is a heterogeneous material consisting of mortar, coarse aggregates, defects, and interface transition zones. The reason for a turning point appears in the load–time curve may be the size and spatial distribution of aggregates, the size and spatial distribution of defects, etc. It would be interesting to explore the factors responsible for a turning point appears in the load–time curve in future research.

Most researchers selected the peak load value to calculate the dynamic tensile strength, which is reasonable when the load–time curve does not present a turning point before the peak load. But it is difficult to calculate the dynamic tensile strength when the load–time curve shows a turning point before the peak load because there is no basis for choosing the load at the turning point or the peak. To select the load value at the turning point or the peak when calculating dynamic tensile strength, it is essential to observe crack initiation of the concrete specimen and obtain the load value when cracks appear.

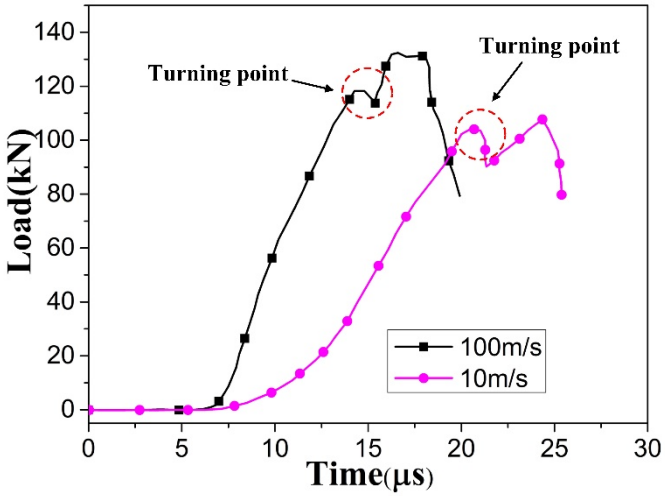

Figure 5. Load–time curves in the dynamic Brazilian disc test at different loading speeds from Ref. [24].

The DIC technology can measure full-field strain and displacement of the surface specimens, including change in displacement at any point and change in distance between two arbitrary points. In Brazilian disc test, the crack initiation should appear near the center of the specimen based on the Griffith fracture criterion, which is apparently supported by numerical and experimental studies [38,39]. In this study, the crack initiation almost always appears near the center of the specimen. Therefore, the center of the concrete specimen is selected as point A, as shown in Figure 6. Point A is the midpoint of points B and C, and the distance between point B and point C is 40 mm, and line AB perpendicular to *X* axis. When the stress wave from the incident bar reaches the concrete specimen, point A will move along the X-direction. In other words, the beginning of the change of displacement at point A means the load starts to be applied to point A. In the dynamic Brazilian disc test, the concrete specimen is finally broken into two halves along the X-direction, and the distance between point B and point C will increase suddenly. The beginning of the change of distance between points A and B implies the concrete specimen begins to crack because concrete is a quasi-brittle material.

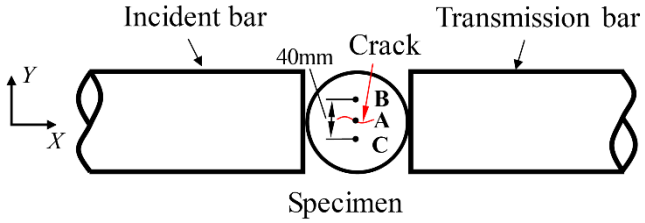

Figure 6. The position of points A, B, and C in the concrete specimen.

The time duration between loading and crack initiation can be measured by the DIC technology. The time duration from zero to the turning point or the peak of the load can be acquired by the load–time curve. It can determine the crack initiation tensile strength of concrete specimens by contrasting the time duration from the DIC technology and the load–time curve. The next step describes how to combine the load–time curve from the dynamic Brazilian disc test with the DIC technology to determine the load value when the concrete specimen displays crack.

3.1. The Concrete Specimen with a Turning Point in the Load–Time Curve

First, the load value of concrete specimen with a turning point in the load–time curve is determined when the cracking first occurs. As shown in Figure 7, the displacement along the X-direction of point A and the distance between points B and C are obtained by

the DIC technology. Before the 8th image, the displacement of point A fluctuates around zero because the stress wave from the incidence bar does not arrive at point A. At the critical point near the 9th image, the displacement of point A suddenly increases from zero because the stress wave reaches point A. For the sake of getting the critical point where the displacement of point A begins to increase from zero, four points from the black ellipse in Figure 7 are selected for linear fitting as in Equation (8). The reason for selecting the four points is they are near the critical point after point A abruptly begins to increase from zero.

$$y_1 = 0.071x - 0.619 \tag{8}$$

where y_1 denotes the displacement of point A, x represents number of images.

Let $y_1 = 0$, the critical point where the load starts to be applied to point A is $x = 8.7$.

At the critical point near the 13th image, the distance between points B and C begins to increase. For the purpose of obtaining the critical point where the distance between points B and C starts to increase from zero, four points from the red ellipse in Figure 7 for linear fitting as in Equation (9).

$$y_2 = 0.17x - 2.221 \tag{9}$$

where y_2 denotes the distance between points B and C, x represents number of images.

Let $y_2 = 0$, the critical point where cracks appear is $x = 13.1$.

The time interval between two adjacent images is about 33.3 μs because the frame frequency of the high-speed cameras is 30,000 fps. The time duration from loading to cracking at point A is $(13.1 - 8.7) \times 33.3$ μs $= 147$ μs. From Figure 4a, it can be seen that the time duration for the load force from zero to the turning point is 157 μs. The time duration for the load force from zero to the peak is 257 μs. It is obvious that the time duration 157 μs which the load force from zero to the turning point is very close to the time duration 147 μs from loading to cracking at point A. The time duration of the load force from zero to the peak is 257 μs, which is much larger than the time duration of 147 μs from loading to crack at point A. It can be concluded that for the concrete specimen with a turning point in the load–time curve, the load force arrives at the turning point when the cracking first occurs.

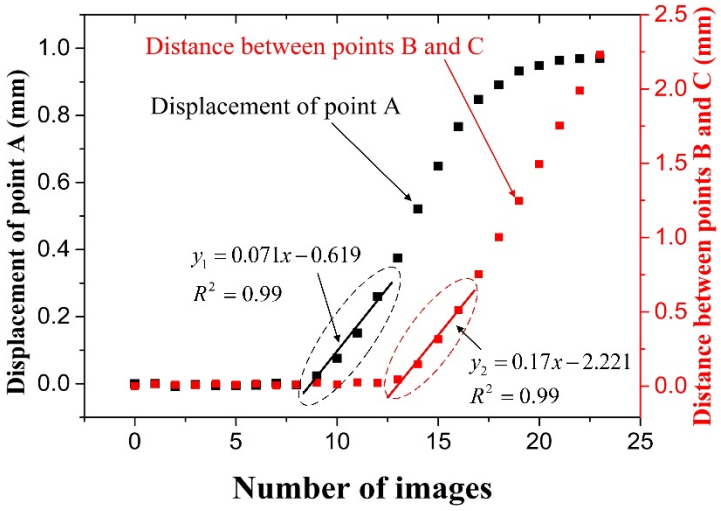

Figure 7. Scatter diagram of displacement change at point A and distance variation between points B and C of the specimen with a turning point in the load–time curve.

3.2. The concrete Specimen without a Turning Point in the Load–Time Curve

When the cracks appear, the load value of the concrete specimen without a turning point in the load–time curve is measured using the method mentioned above.

For the sake of getting the critical point in which the displacement of point A begins to increase from zero, four points from the black ellipse in Figure 8 for linear fitting as in Equation (10).

$$y_1 = 0.08x - 0.324 \tag{10}$$

where y_1 denotes the displacement of point A, x represents number of images.

Let $y_1 = 0$, the critical point where the load starts to be applied to point A is $x = 4.1$.

To obtain the critical point where the distance between points B and C starts to increase from zero, four points from the red ellipse in Figure 8 for linear fitting as in Equation (11).

$$y_2 = 0.131x - 1.323 \tag{11}$$

where y_2 denotes the distance between points B and C, x represents number of images.

Let $y_2 = 0$, the critical point at which crack occur is $x = 10.1$.

The time duration from loading to cracking at point A is $(10.1 - 4.1) \times 33.3\ \mu s = 200\ \mu s$. From Figure 3a, it can be seen that the time duration for the load force from zero to the peak is 182 μs. The time duration of the load force from zero to the peak is 182 μs, which is very close to the time duration of 200 μs from loading to crack at point A. The time duration 200 μs − 182 μs = 18 μs is less than the time interval of 33.3 μs between two adjacent images. It can be concluded that for the concrete specimen without a turning point in the load–time curve, the load force arrives at the peak when the cracking first appears.

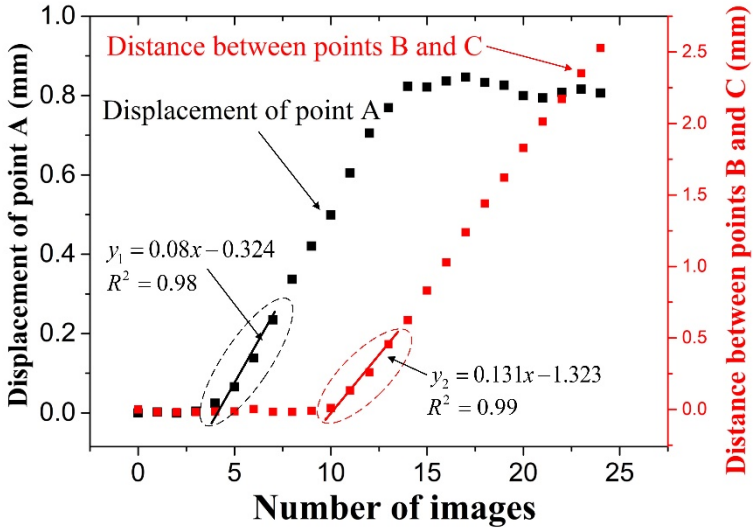

Figure 8. Scatter diagram of displacement change at point A and distance variation between points B and C of the specimen without a turning point in the load–time curve.

4. Results and Discussions

4.1. The Crack Evolution

The DIC technology can obtain the crack evolution of concrete specimens in dynamic Brazilian disc tests. The proposed method can find the relation between the crack evolution and the load–time curve.

For the concrete specimen with a turning point in the load–time curve, the cracks appear at the 13.1th image according to the DIC technology, and the cracks occur at the 157th microsecond based on the load–time curve. The 13th image will occur at $157 - (13.1 - 13) \times 33.3 = 154$th microsecond in the load–time curve. It is easy to find the point at the 154th microsecond in Figure 9, where the 13th image appears exactly. The 14th image is found by starting at the 154th microsecond and moving 33.3 microsecond to the right. Through this method, the rest of the images can be found in Figure 9.

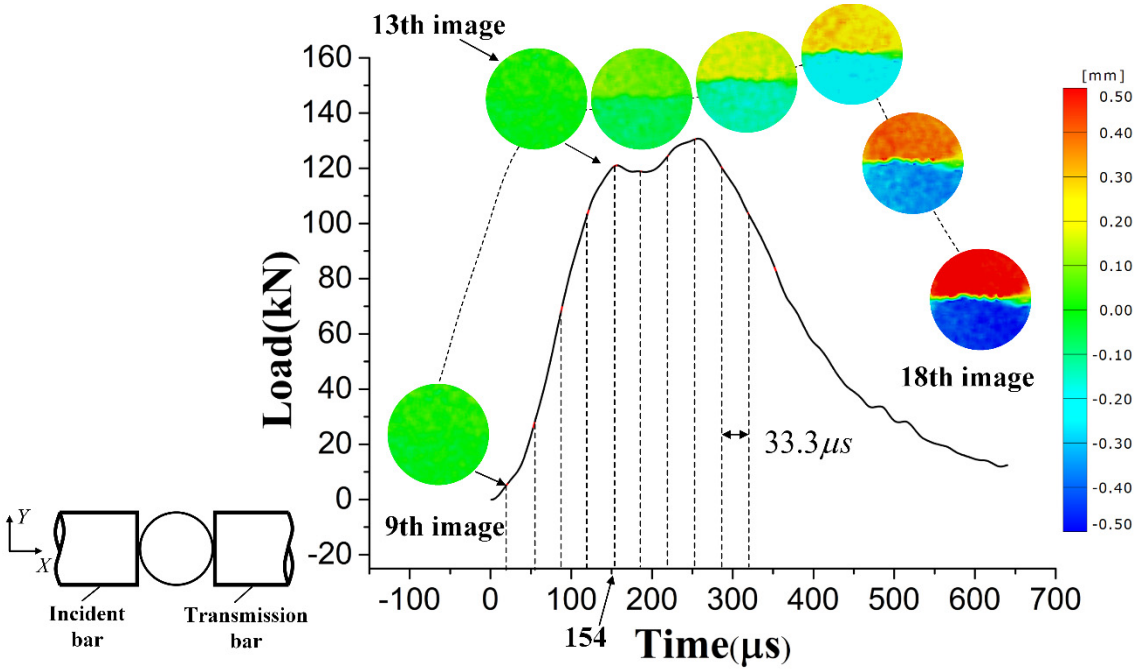

Figure 9. The relation between the images from the high-speed camera and the load–time curve with a turning point.

Figure 9 shows the Y-direction displacement of the concrete specimen surface. The Y-direction displacement before the 13th image and the 13th image is almost zero. The Y-direction displacement in the 14th image begins to change abruptly. This phenomenon indicates crack initiation between the 13th image and the 14th image.

The DIC technology can acquire Y-direction strain, as shown in Figure 10. Cracks appear abruptly in the 14th image. Cracks expand along X-direction with increasing loading force. The concrete specimen eventually breaks into two halves.

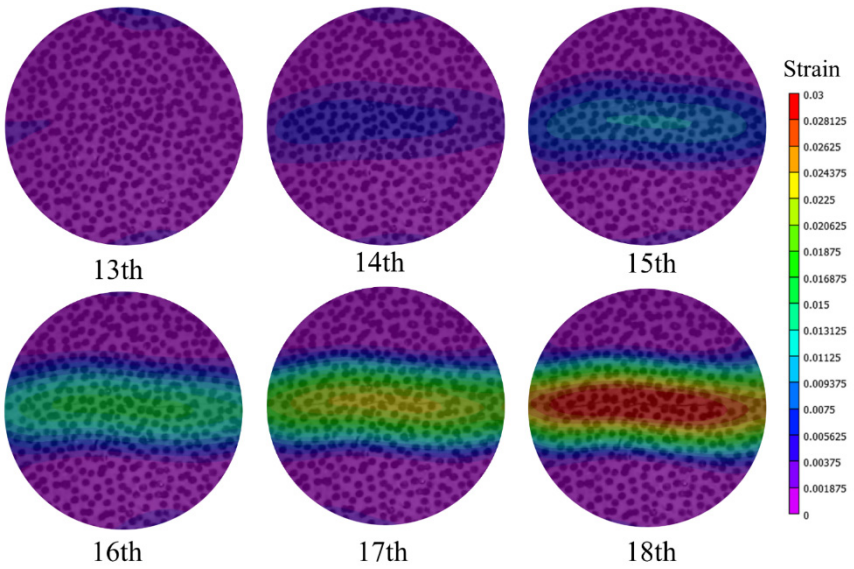

Figure 10. Strain variation diagram of concrete specimen with a turning point in the load–time curve.

For the concrete specimen without a turning point in the load–time curve, the cracks occur at the 10.1th image according to the proposed method, and the cracks appear at the 182th microsecond based on the load–time curve. The 10th image will occur at $182 - (10.1 - 10) \times 33.3 = 179$th microsecond in the load–time curve. It is easy to find the

point at 179th microsecond in Figure 11, where the 10th image appears exactly. The 11th image is found by starting at the 156th microsecond and moving 33.3 microsecond to the right. Through this method, the rest of the images can be found in Figure 11. Figure 11 shows the Y-direction displacement of the concrete specimen without a turning point in the load–time curve.

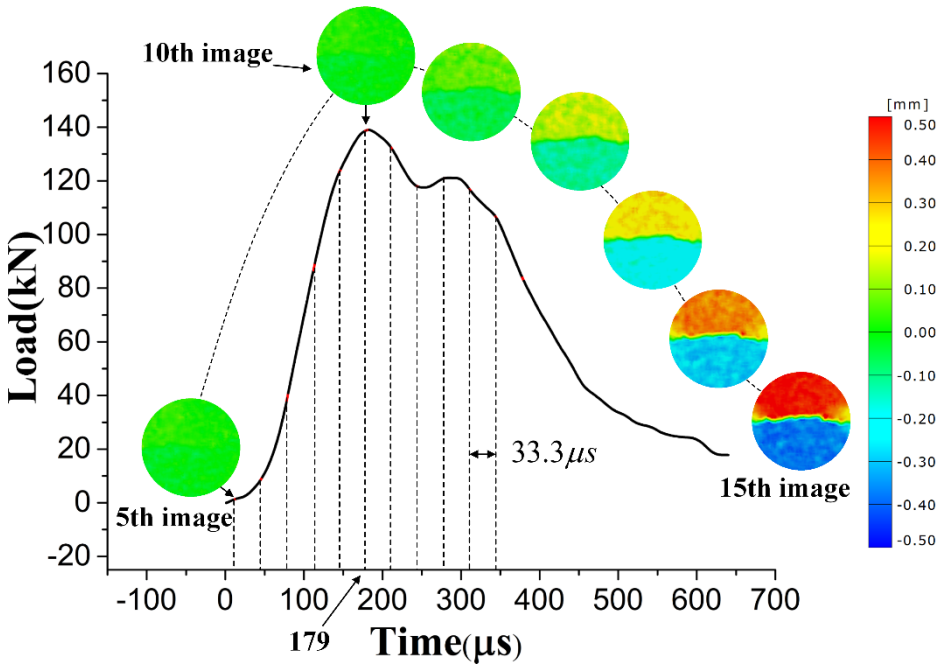

Figure 11. The relation between the images from the high-speed cameras and the load–time curve without a turning point.

The DIC technology can acquire the Y-direction strain of the concrete specimen without a turning point in the load–time curve, as shown in Figure 12. By comparing Figures 10 and 12, it can be seen that the cracks appear from the center of the concrete specimens, and they propagate toward both ends of the specimens as the load increases. This indicates the turning point in the load–time curve is little influential to the crack evolution modes of the concrete specimens in the dynamic Brazilian disc test.

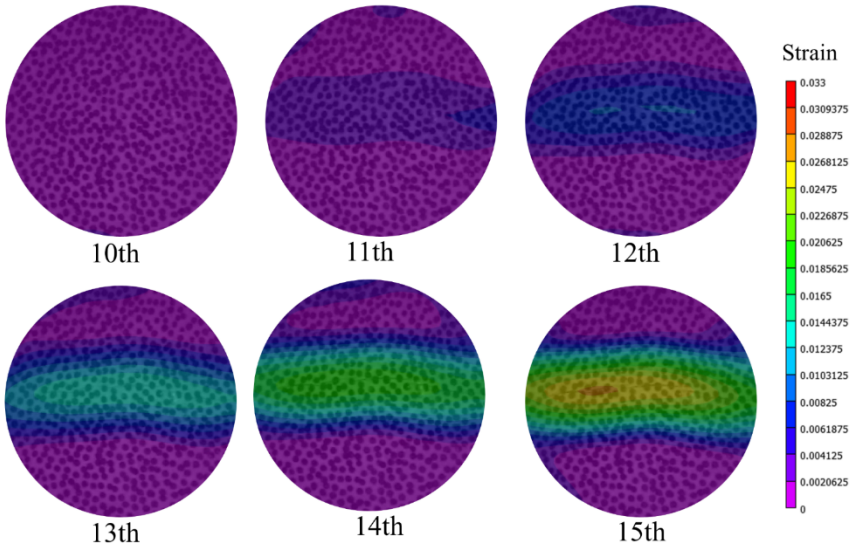

Figure 12. Strain variation diagram of concrete specimen without a turning point in the load–time curve.

4.2. The Tensile Strength at Crack Initiation

This study proposes a method to determine the load value when cracks occur. For the concrete specimen with a turning point in the load–time curve, the cracks appear when the load force arrives at the turning point, crack initiation tensile strength can be calculated by the load arriving at the turning point, and the peak tensile strength can be calculated by the peak load value. For the concrete specimen without a turning point in the load–time curve, the cracks appear when the load force arrives at its peak value, the crack initiation tensile strength and the peak tensile strength can be calculated by the peak load. The tensile strength of concrete includes the crack initiation tensile strength and the peak tensile strength in Table 2, which is calculated by Equation (7).

Table 2. The crack initiation tensile strength and the peak tensile strength of the concrete specimens.

Specimen Type		Load (kN)		Tensile Strength (MPa)		Ratio (%)
		Crack Initiation	Peak	Crack Initiation	Peak	
The load–time curve with a turning point	N-2	121.21	130.82	6.43	6.94	107.9
	N-6	126.28	134.45	6.70	7.14	106.5
	N-10	102.84	145.81	5.46	7.74	141.8
The load–time curve with no turning point	N-1	138.96	138.96	7.38	7.38	100.0
	N-3	142.26	142.26	7.55	7.55	100.0
	N-4	129.98	129.98	6.90	6.90	100.0
	N-5	143.34	143.34	7.61	7.61	100.0
	N-7	135.51	135.51	7.19	7.19	100.0
	N-8	136.27	136.27	7.23	7.23	100.0
	N-9	144.14	144.14	7.65	7.65	100.0

Table 2 shows that the ratio of the peak tensile strength to the crack initiation tensile strength of the concrete specimens. For the concrete specimens without a turning point in the load–time curve, a total of seven specimens of the crack initiation tensile strength is equal to the peak tensile strength. For the concrete specimens with a turning point in the load–time curve, the crack initiation tensile strength of a total of three specimens is less than the peak strength, and the maximum difference between them is about 41.8%. In summary, the crack initiation tensile strength is less than or equal to the peak tensile strength of concrete specimens.

5. Conclusions

The DIC technology can acquire the time duration from loading to cracking of concrete specimen. The time duration from zero to the turning point or the peak of the load can be obtained by the load–time curve. The proposed method contrasts the time duration from the DIC technology and the load–time curve, obtains the load force when cracks appear, and find the relation between the crack evolution and the load–time curve. Using this method, the following conclusions can be drawn.

The tensile strength of concrete includes the crack initiation tensile strength and the peak tensile strength in the dynamic Brazilian disc test. For concrete specimens with a turning point in the load–time curve, cracks occur at the turning point, the crack initiation tensile strength is less than the peak strength, and the maximum difference between them is about 41.8%. For concrete specimens without a turning point in the load–time curve, cracks appear at the peak load value, and crack initiation tensile strength is equal to the peak strength. The crack initiation tensile strength is less than or equal to the peak tensile strength of concrete specimens. It is more reasonable and safer to choose the crack initiation tensile strength as tensile strength of concrete in the dynamic Brazilian disc test.

In the dynamic Brazilian disc test, cracks appear from the center of the concrete specimens, and the cracks propagate toward both ends of the specimens with the increase of loading. The presence or absence of the turning point in the load–time curve is little influential to the crack evolution modes of the concrete specimens.

The proposed method has proven to be successful in determining the crack initiation tensile strength of concrete. It can also be applied in the dynamic Brazilian disc test to determine the crack initiation tensile strength of other brittle materials involving sandstone, marble, etc.

Author Contributions: Conceptualization, investigation, data curation writing—original draft, J.W.; methodology, supervision, review, J.T. All authors have read and agreed to the published version of the manuscript.

Funding: This research received no external funding.

Institutional Review Board Statement: Not application.

Informed Consent Statement: Not application.

Data Availability Statement: Data available on request from the authors.

Conflicts of Interest: The authors declare no conflict of interest.

References

1. Ning, J.; Wang, J.; Jiang, J.; Hu, S.; Jiang, L.; Liu, X. Estimation of Crack Initiation and Propagation Thresholds of Confined Brittle Coal Specimens Based on Energy Dissipation Theory. *Rock Mech. Rock Eng.* **2018**, *51*, 119–134. [CrossRef]
2. Brace, W.F.; Paulding, B.W.; Scholz, C., Jr. Dilatancy in the fracture of crystalline rocks. *J. Geophys. Res.* **1966**, *71*, 3939–3953. [CrossRef]
3. Ündül, O.; Amann, F.; Aysal, N.; Plötze, M.L. Micro-textural effects on crack initiation and crack propagation of andesitic rocks. *Eng. Geol.* **2015**, *193*, 267–275. [CrossRef]
4. Lajtai, E. Brittle fracture in compression. *Int. J. Fract.* **1974**, *10*, 525–536. [CrossRef]
5. Martin, C.D.; Chandler, N.A. The progressive fracture of Lac du Bonnet granite. *Int. J. Rock Mech. Min. Sci. Geomech. Abstr.* **1994**, *31*, 643–659. [CrossRef]
6. Nicksiar, M.; Martin, C.D. Evaluation of Methods for Determining Crack Initiation in Compression Tests on Low-Porosity Rocks. *Rock Mech. Rock Eng.* **2012**, *45*, 607–617. [CrossRef]
7. Wen, T.; Tang, H.; Ma, J.; Wang, Y. Evaluation of methods for determining crack initiation stress under compression. *Eng. Geol.* **2018**, *235*, 81–97. [CrossRef]
8. Eberhardt, E.; Stead, D.; Stimpson, B.; Read, R. Identifying crack initiation and propagation thresholds in brittle rock. *Can. Geotech. J.* **1998**, *35*, 222–233. [CrossRef]
9. Pepe, G.; Mineo, S.; Pappalardo, G.; Cevasco, A. Relation between crack initiation-damage stress thresholds and failure strength of intact rock. *Bull. Eng. Geol. Environ.* **2018**, *77*, 709–724. [CrossRef]
10. Li, X.F.; Li, H.; Liu, L.; Liu, Y.; Ju, M.; Zhao, J. Investigating the crack initiation and propagation mechanism in brittle rocks using grain-based finite-discrete element method. *Int. J. Rock Mech. Min. Sci.* **2020**, *127*, 104219. [CrossRef]
11. Rocco, C.; Guinea, G.; Planas, J.; Elices, M. Review of the splitting-test standards from a fracture mechanics point of view. *Cem. Concr. Res.* **2001**, *31*, 73–82. [CrossRef]
12. Xu, Y.; Dai, F.; Zhao, T.; Xu, N.-W.; Liu, Y. Fracture Toughness Determination of Cracked Chevron Notched Brazilian Disc Rock Specimen via Griffith Energy Criterion Incorporating Realistic Fracture Profiles. *Rock Mech. Rock Eng.* **2016**, *49*, 3083–3093. [CrossRef]
13. Chen, C.-S.; Pan, E.; Amadei, B. Fracture mechanics analysis of cracked discs of anisotropic rock using the boundary element method. *Int. J. Rock Mech. Min. Sci.* **1998**, *35*, 195–218. [CrossRef]
14. Sun, W.; Wu, S. A study of crack initiation and source mechanism in the Brazilian test based on moment tensor. *Eng. Fract. Mech.* **2021**, *246*, 107622. [CrossRef]
15. Guo, H.; Tao, J.; Chen, Y.; Li, D.; Jia, B.; Zhai, Y. Effect of steel and polypropylene fibers on the quasi-static and dynamic splitting tensile properties of high-strength concrete. *Constr. Build. Mater.* **2019**, *224*, 504–514. [CrossRef]
16. Aliabadian, Z.; Zhao, G.-F.; Russell, A.R. Failure, crack initiation and the tensile strength of transversely isotropic rock using the Brazilian test. *Int. J. Rock Mech. Min. Sci.* **2019**, *122*, 104073. [CrossRef]
17. Sharafisafa, M.; Aliabadian, Z.; Shen, L. Crack initiation and failure of block-in-matrix rocks under Brazilian test using digital image correlation. *Theor. Appl. Fract. Mech.* **2020**, *109*, 102743. [CrossRef]
18. Cai, M. Practical Estimates of Tensile Strength and Hoek–Brown Strength Parameter mi of Brittle Rocks. *Rock Mech. Rock Eng.* **2010**, *43*, 167–184. [CrossRef]
19. Wang, Q.Z.; Yang, J.; Zhang, C.; Zhou, Y.; Li, L.; Zhu, Z.; Wu, L. Sequential determination of dynamic initiation and propagation toughness of rock using an experimental–numerical–analytical method. *Eng. Fract. Mech.* **2015**, *141*, 78–94. [CrossRef]
20. Zhou, Z.L.; Li, X.B.; Zou, Y.; Jiang, Y.H.; Li, G.N. Dynamic Brazilian Tests of Granite Under Coupled Static and Dynamic Loads. *Rock Mech. Rock Eng.* **2014**, *47*, 495–505. [CrossRef]

21. Ai, D.H.; Zhao, Y.C.; Xie, B.; Li, C.W. Experimental Study of Fracture Characterizations of Rocks under Dynamic Tension Test with Image Processing. *Shock Vib.* **2019**, *2019*, 6352609. [CrossRef]
22. Chen, J.J.; Guo, B.Q.; Liu, H.B.; Liu, H.; Chen, P.W. Dynamic Brazilian Test of Brittle Materials Using the Split Hopkinson Pressure Bar and Digital Image Correlation. *Strain* **2014**, *50*, 563–570. [CrossRef]
23. Wu, R.J.; Li, H.B.; Wang, D.P. Full-field deformation measurements from Brazilian disc tests on anisotropic phyllite under impact loads. *Int. J. Impact Eng.* **2021**, *149*, 103790. [CrossRef]
24. Ruiz, G.; Ortiz, M.; Pandolfi, A. Three-dimensional finite-element simulation of the dynamic Brazilian tests on concrete cylinders. *Int. J. Numer. Methods Eng.* **2000**, *48*, 963–994. [CrossRef]
25. Liu, P.; Zhou, X.; Qian, Q.; Berto, F.; Zhou, L. Dynamic splitting tensile properties of concrete and cement mortar. *Fatigue Fract. Eng. Mater. Struct.* **2020**, *43*, 757–770. [CrossRef]
26. China Academy of Building Research. *Specification for Mix Proportion Design of Ordinary Concrete*; China Architecture & Building Press: Beijing, China, 2011.
27. Sharafisafa, M.; Aliabadian, Z.; Shen, L. Crack initiation and failure development in bimrocks using digital image correlation under dynamic load. *Theor. Appl. Fract. Mech.* **2020**, *109*, 102688. [CrossRef]
28. Szewczyk, P.; Kudyba, P. Effectiveness of Selected Strain and Displacement Measurement Techniques in Civil Engineering. *Buildings* **2022**, *12*, 172. [CrossRef]
29. Beßling, M.; Czaderski, C.; Orlowsky, J. Prestressing Effect of Shape Memory Alloy Reinforcements under Serviceability Tensile Loads. *Buildings* **2021**, *11*, 101. [CrossRef]
30. Pan, B. Digital image correlation for surface deformation measurement: Historical developments, recent advances and future goals. *Meas. Sci. Technol.* **2018**, *29*, 082001. [CrossRef]
31. Pan, B.; Qian, K.; Xie, H.; Asundi, A. Two-dimensional digital image correlation for in-plane displacement and strain measurement: A review. *Meas. Sci. Technol.* **2009**, *20*, 62001. [CrossRef]
32. Li, X.; Wang, S.; Xia, K.; Tong, T. Dynamic Tensile Response of a Microwave Damaged Granitic Rock. *Exp. Mech.* **2021**, *61*, 461–468. [CrossRef]
33. Ma, H.B.; Yang, S.F.; Xu, Y.; Chen, P.Y.; Wang, L. Dynamic Mechanical Properties of Slag Mortar with Alkali-Resistant Glass Fiber. *Buildings* **2022**, *12*, 266. [CrossRef]
34. Lindholm, U. Some experiments with the split hopkinson pressure bar*. *J. Mech. Phys. Solids* **1964**, *12*, 317–335. [CrossRef]
35. *Standard Test Method for Splitting Tensile Strength of Cylindrical Concrete Specimens*; ASTM International: West Conshohocken, PA, USA, 2011.
36. Gomez, J.; Shukla, A.; Sharma, A. Static and dynamic behavior of concrete and granite in tension with damage. *Theor. Appl. Fract. Mech.* **2001**, *36*, 37–49. [CrossRef]
37. Guo, Y.B.; Gao, G.F.; Jing, L.; Shim, V.P.W. Quasi-static and dynamic splitting of high-strength concretes—tensile stress–strain response and effects of strain rate. *Int. J. Impact Eng.* **2019**, *125*, 188–211. [CrossRef]
38. Chen, S.; Yue, Z.Q.; Tham, L.G. Digital image-based numerical modeling method for prediction of inhomogeneous rock failure. *Int. J. Rock Mech. Min. Sci.* **2004**, *41*, 939–957. [CrossRef]
39. Yanagidani, T.; Sano, O.; Terada, M.; Ito, I. The observation of cracks propagating in diametrically-compressed rock discs. *Int. J. Rock Mech. Min. Sci. Geomech. Abstr.* **1978**, *15*, 225–235. [CrossRef]